

## Plastic Deformation of High Explosive Projectile 155 mm during Gun Launch Conditions using Finite Element Method

Rajesh B. Ohol,<sup>#,\*</sup> B.A. Parate<sup>§</sup> and Dineshsingh G. Thakur<sup>#</sup>

<sup>#</sup>DRDO - Defence Institute of Advanced Technology (DIAT), Deemed University, Pune - 411 025, India

<sup>§</sup>DRDO - Armament Research and Development Establishment (ARDE), Pune - 411 021, India

\*E-mail: ohol\_rajesh@yahoo.com

### ABSTRACT

The structural integrity of artillery projectile 155mm high explosive Extended Range Full Bore (ERFB) boat tail designed for 155mm howitzer guns of 39, 45 and 52 calibre plays a key role inside the gun barrel. This projectile comprises a shell body, a driving band, a boat tail, nubs, an explosive, and a fuze. Plastic deformation of the projectile and stripping of driving band are not permitted, when projectile is fired. An investigational study is necessitated to check the plastic deformation of the projectile subjected to maximum propellant charge pressure. The aim of this study is to check the effective plastic deformation and affirm the structural integrity. A 3-D explicit dynamic structural analysis of 155 mm HE ERFB BT during gun launch conditions is carried out by finite element method using FE code ABAQUS/Explicit. To understand the non-linear mechanical behavior of the projectile, the true stress-strain curves of the materials are considered. The plastic behavior of the projectile subjected to the time-dependent loading is studied by using the von Mises plasticity model. The results reveal that the shell body and boat tail have no plastic deformation and the most stressed component is the driving band. The investigation has affirmed the structural integrity of the projectile during gun launch conditions.

**Keywords:** 155 mm HE ERFB BT; Explicit dynamic analysis; Internal ballistics; Plastic deformation; Structural integrity

### 1. INTRODUCTION

155 mm high explosive Extended Range Full Bore (ERFB) boat tail is a chemical energy projectile, which is fired from 39, 45 and 52 calibre 155 mm artillery guns. It is deployed for the rapid and accurate firing at long ranges to attack the ground targets. 155 mm HE ERFB BT projectile comprises a shell body, a driving band, a boat tail, nubs, trinitrotoluene (TNT) explosive and a fuze or a recovery plug as its components. The projectile has the shape of a cylindrical shell with an extended front ogive. The four nubs are Metal Inert Gas (MIG) welded on the front portion of ogive. The nubs act as bourrelet, thus providing the support to launch stability. Upon firing, the driving band engraves into the lands and grooves of the barrel and imparts spin to the projectile. An aluminum alloy body of the boat tail unit is threaded to the bottom of the shell body. During flight, it reduces base drag thereby enhancing the range of the projectile. An electronic point detonating fuze with an immediate and/or delay function is screwed into the nose cavity of the shell.

155 mm ERFB boat tail is a spin-stabilized projectile with an axisymmetric cylindrical shell shape. Spin and acceleration gained by the projectile upon firing give rise to the loads on the shell body. The stresses encountered vary along and through the wall of the shell body. The shell body assembly has to

withstand the firing stresses. These stresses are examined as the consequences of failure criteria.<sup>1</sup> Designing a projectile must ensure that it is capable of surviving gun launch conditions.<sup>2</sup>

Bursting of the shell inside the gun barrel on account of firing stresses is a critical defect leading to a catastrophic accident. A projectile may fail structurally either in a plastic mode or a brittle mode. Plastic failure occurs when sections of the projectile undergo such large plastic deformations that they can no longer transmit the applied load. Brittle failure occurs when a flaw is stressed to a level where it propagates unstably<sup>3</sup>.

The plastic deformation of the shell body during the launch inside the gun is not acceptable from the point of view of the integrity and strength of the shell body material.<sup>4-5</sup> The unintended ignition of a high explosive projectile during gun launch occurs depending upon the setback sensitivity of the defects such as cracks, voids, porosity, foreign material, base gaps, piping, migration and exudation of projectile explosive filling.<sup>6-7</sup> Special mechanical events are required for ignition to occur. Mechanical behavior of the projectile in gun bore is affected by various parameters like launch loads including launch accelerations, rotating band pressure, gas pressure on the projectile case, and centripetal acceleration.<sup>8</sup> Tsui,<sup>9</sup> *et al.* applied 3-D elastic plastic dynamic approach for stress analysis of a spline joint of XM785 projectile. This finite element analysis covered the joint portion of the projectile only disregarding the true stress-strain curves of the materials.

Pflegl<sup>10</sup> *et al.*, Hollis<sup>11</sup>, Phatak<sup>12</sup> *et al.* performed 2D axisymmetric structural analyses of the Kinetic Energy (KE) projectile with the help of finite element method for verifying in-bore structural integrity of KE projectile. These finite element structural analyses disregarded non-linear behavior of the projectile. Balasubramanian,<sup>13</sup> *et al.* undertook the investigational study on the failure of 125 mm tank gun barrel owing to ingress of sand particles during firing with High Explosive Fragmentation (HEF) projectile. Finite Element Analysis (FEA) was carried out to investigate the failure of gun barrel with the presence of sand deposits. The study focused on the effect of the presence of foreign material inside the gun barrel. Accordingly, the stress analysis of the gun barrel was studied. At the same time, failure of the gun barrel on account of structural failure of the projectile cannot be ruled out at the peak propellant pressure.

Bender,<sup>14</sup> *et al.* used the finite element analysis technique for the assessment of the structural integrity of the Excalibur 155mm Artillery Shell's Canard Activation System. This structural analysis study is confined to a unit of Excalibur projectile. Brett<sup>15</sup> carried out a quasi-static computation of KE projectile by assuming that though the propellant pressure rises in a very short time, the shear wave propagation in the elastic material is not significant as per the dynamic analyses.

Of late, a number of studies have been made for static structural analysis of KE as well as chemical energy projectiles considering the elasticity of projectile material. The review of the existing literature shows that most of structural analyses were carried out for chemical energy projectiles using 2-D axis symmetric approach, providing the limited data on non-linear 3-D dynamic structural analysis of high explosive projectile subjected to the dynamic firing system. The mechanical behavior of shell 155 mm high explosive ERFB boat tail seems to be more studied from the point of view of plasticity of the shell assembly. This study aims to check the effective plastic deformation of the shell body, boat tail and driving band materials during gun launch conditions and affirm the structural integrity by performing the non-linear structural analysis using finite element method.

For the present analysis study, the projectile experiences a maximum gun chamber pressure of 404 MPa and an acceleration of 13694 g, when propelling charge Bi-Modular Charge System (BMCS) for high zone-6 for 45 calibre gun is employed during the firing. The uniaxial tensile tests of the specimens prepared from the shell body, boat tail and driving band materials are carried out as per the standard ASTM E8.<sup>16</sup> The true stress-strain curves based on the experimental data and the pressure-time curve obtained from the dynamic firing are used in the 3-D explicit dynamic non-linear structural analysis carried out in ABAQUS/ Explicit. The plastic deformation of shell 155mm high explosive ERFB boat tail is analyzed.

## 2. METHODS AND MATERIALS

Finite element analysis can model complex conditions and handle the quasi-static, implicit dynamic and explicit dynamic analyses of shell assembly during gun launch conditions. A

commercial software ABAQUS 2020 is used for the present analysis. ABAQUS/Explicit based on explicit integration rule is selected for the nonlinear analysis.

### 2.1 Geometric Model

A 3-D model of the high explosive filled 155 mm ERFB boat tail given in Fig. 1 was generated in Solid Works and used as an input file for meshing and loading in ABAQUS. For the current 3-D explicit dynamic structural non-linear analysis, material and geometric non-linearities, also constraints and interaction between the surface with friction properties at threads between boat tail and the shell body, recovery plug and the shell body as well as joints between nubs and the shell body were selected.

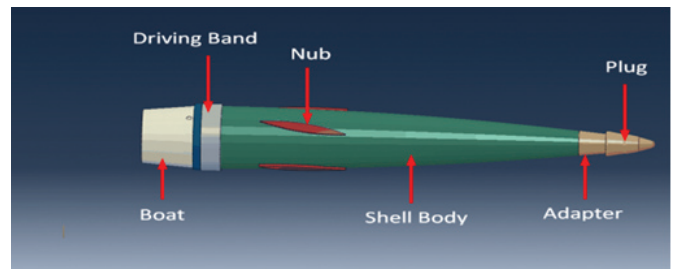


Figure 1. A 3-D model of high explosive filled 155 mm ERFB BT.

### 2.2 Meshing

Structured and swept meshing techniques of 3-D model with 3-D, 8-node linear hexahedral solid element with reduced integration (C3D8R) were used for equivalent accuracy. Figure 2 shows the meshed 3-D model of projectile 155mm HE ERFB BT. C3D8R element is an 8 node linear brick element with reduced integration. The total number of elements used was 3,21,539. This type of element facilitates fast computation with reduced calculation on account of lesser integration points. For the stress/displacement problems, the significant accuracy is obtained using this type of element. To ensure mesh convergence, the model was meshed properly with fine mesh.

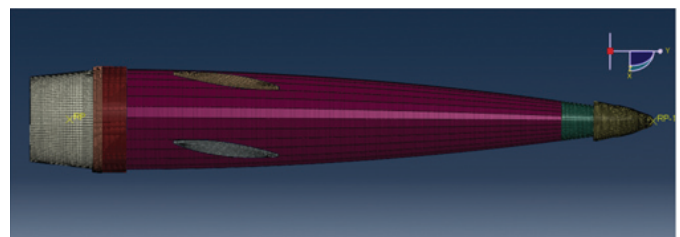


Figure 2. A meshed 3-D model of 155 mm HE ERFB BT.

### 2.3 Material Model

To obtain realistic plastic behavior of the shell body of the projectile, non-linearity of material, geometry and contacts was included in the present analysis. The material details of components of the projectile 155mm ERFB boat tail are given in Table 1.

**Table 1. Material details of projectile 155 mm ERFB BT**

Component	Material	Yield strength (MPa)	Poisson's ratio	Modulus of elasticity (GPa)	Density (g/cm <sup>3</sup> )
Shell Body	Alloy Steel	780	0.29	200	7.8
Boat Tail	Al Alloy	435	0.33	71	2.82
Nub	Carbon Steel	0.2% Proof Stress 240	0.33	200	7.8
Driving Band	Copper Alloy	90	0.285	121	8.98
Explosive Filling	TNT	58	0.36	4.2	1.7
Plug & Adaptor	En 8	465	0.27	200	7.87

## 2.4 Uniaxial Tensile Tests

The engineering stress-strain curve does not provide a realistic picture of the deformation pattern of material. Hence, the values of stress and strain based on the instantaneous dimensions were used in this explicit dynamic analysis. The conversion of an engineering stress-strain curve into a true stress-strain curve was done for all the materials using the known relations given as under:

$$\varepsilon = \ln(e+1) \quad (1)$$

where,  $\varepsilon$  is true strain and  $e$  is conventional or engineering strain.

$$\sigma = s(e+1) \quad (2)$$

where,  $\sigma$  is true stress and  $s$  is conventional or engineering stress.

Uniaxial tensile tests were carried out on the specimens made out of shell body, boat tail and driving band at quasi-static strain rate at ambient temperature as per the standard ASTM E8. The tensile test specimens six each from shell body, boat tail and driving band materials were prepared. The specimens are shown in Figs. 3, 4 and 5 respectively. The specimens were tested on Universal Testing Machine, Model: HA-100, Capacity: 100kN, Make: Zwick Roell. The experimental set up is shown in Figure 6.

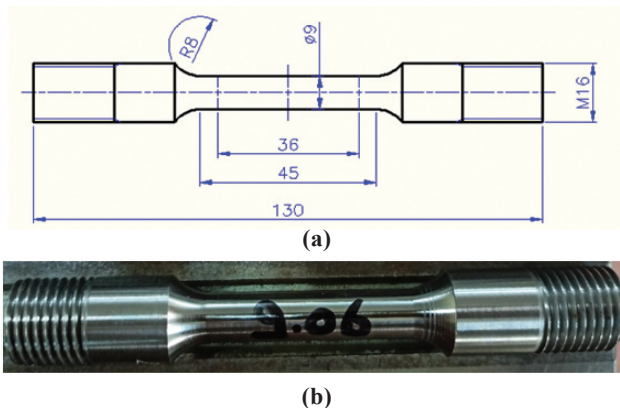


**Figure 3. Shell body material: (a) Tensile test specimen geometry, and (b) Machined specimen.**

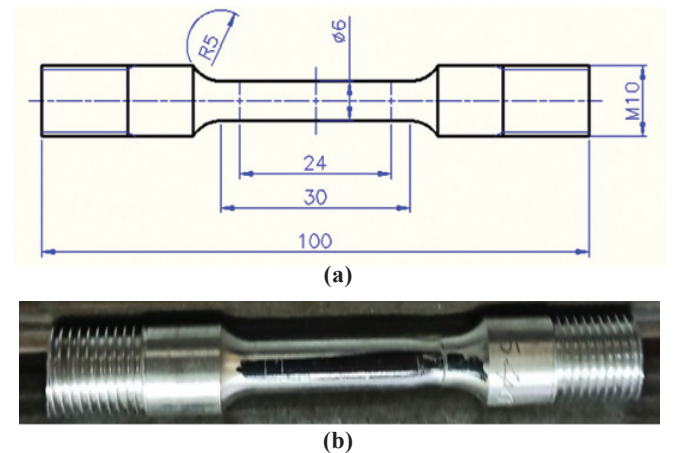


**Figure 4. Boat tail material: (a) Tensile test specimen geometry, and (b) Machined specimen.**

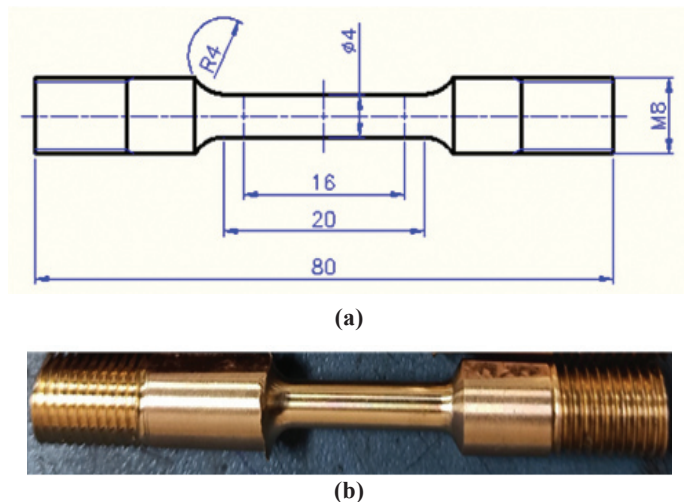


**Figure 5. Driving band material: (a) Tensile test specimen geometry, and (b) Machined specimen.**

Taking into account the average values of stress-strain values obtained from the uniaxial tensile tests, the engineering stress - strain and the true stress - strain curves of the shell body, boat tail and driving band specimens are plotted as shown in Figs.7 (a), (b) & (c) respectively.

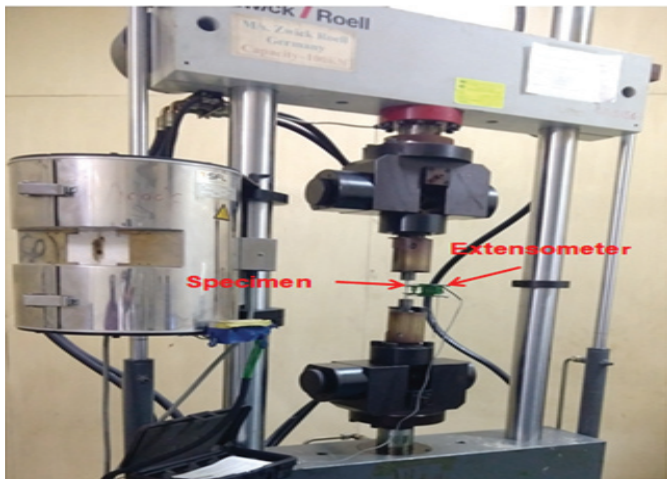
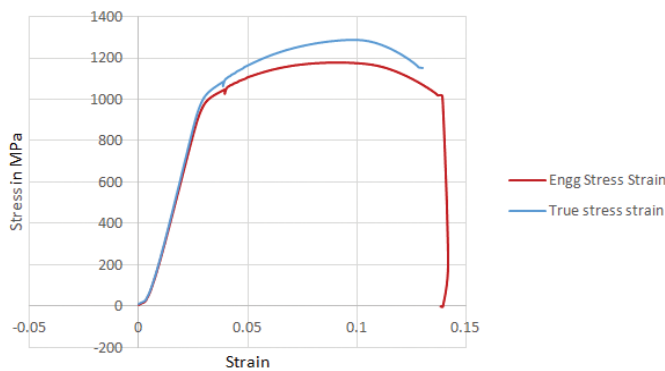
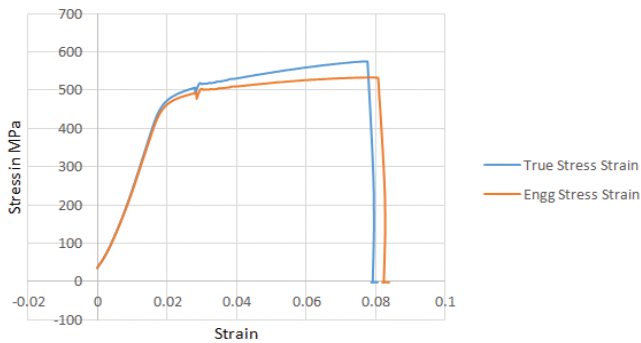


Figure 6. Experimental setup: Universal testing machine with specimen and extensometer.

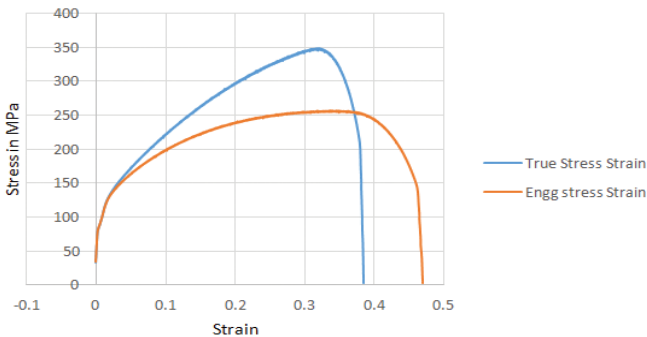


(a)

Stress Vs Strain



(b)



(c)

Figure 7. Engineering stress-strain and the true stress-strain curves: (a) Shell body, (b) Boat tail, and (c) Driving band.

### 2.5 Equivalent Stress and Equivalent Strain

Considering a complex stress condition during gun launch and the material of the shell body, the driving band and the boat tail being ductile, the von Mises or Distortion Energy criterion was applied to understand the effective deformation of the projectile. The conversion of a uniaxial stress state into a multiaxial stress condition is accomplished by the use of the equivalent stress and strain.<sup>17</sup>

The von Mises expressions for equivalent stress ( $\bar{\sigma}$ ) and equivalent strain ( $\bar{\epsilon}$ ) are represented as under:

$$(\bar{\sigma}) = \sqrt{\frac{1}{2} [(\sigma_1 - \sigma_2)^2 + (\sigma_2 - \sigma_3)^2 + (\sigma_3 - \sigma_1)^2]} \quad (3)$$

where,  $\sigma_1$ ,  $\sigma_2$  and  $\sigma_3$  are the principal stresses.

$$(\bar{\epsilon}) = \frac{1}{3} \sqrt{2 [(\epsilon_1 - \epsilon_2)^2 + (\epsilon_2 - \epsilon_3)^2 + (\epsilon_3 - \epsilon_1)^2]} \quad (4)$$

where,  $\epsilon_1$ ,  $\epsilon_2$  and  $\epsilon_3$  are the principal strains.

### 2.6 Yield Criterion

Here, von Mises equivalent stress ( $\bar{\sigma}$ ) is taken as effective stress. When von Mises equivalent stress ( $\bar{\sigma}$ ) is equal to or exceeds the yield tensile strength value  $\sigma_{yt}$ , the material is regarded as yielded.

$$(\bar{\sigma}) \geq \sigma_{yt} \quad (5)$$

### 2.7 Boundary Conditions

The boundary conditions consistent with those from the projectile during the gun-launch environment were applied to the finite element model of the projectile 155mm HE ERFB BT. Accordingly, the projectile rotational and translational motions were restrained at the driving band as shown in Fig. 8.

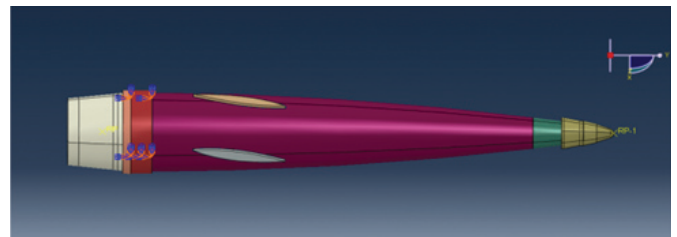


Figure 8. Boundary conditions: Rotational and translational motions restrained at driving band.

### 2.8 Loadings

For the current study, the time-dependent loading based on the pressure-time curve was applied to the projectile. The pressure-time data obtained from the dynamic firing results were inputted for the explicit dynamic analysis. Figure 9 shows the pressure-time ( $P-t$ ) curve of 155mm ERFB BT. The base pressure on the projectile was considered by applying Lagrange approximation.<sup>18</sup> The net pressure on the base of the projectile was calculated taking into account the resistive pressure of the gun barrel<sup>19</sup>.

The force balance of the system was effected by the constraining motion of the projectile at the driving band in axial and radial directions. During the dynamic loading, the

peak net propellant pressure on the base of the projectile and the corresponding spin of the projectile attain the values 323 MPa and 790 rad/s respectively. The dynamic loadings applied on the projectile are shown in Figs. 10(a) and (b).

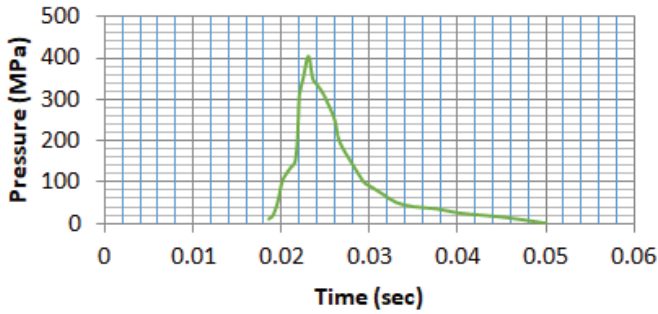
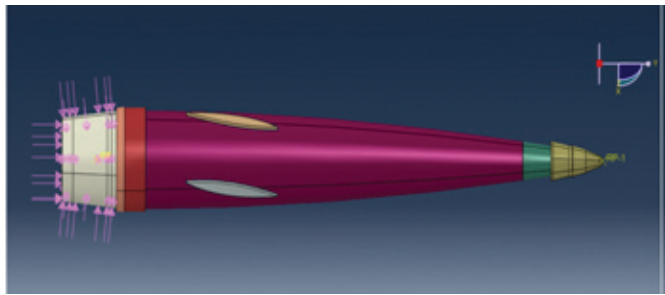
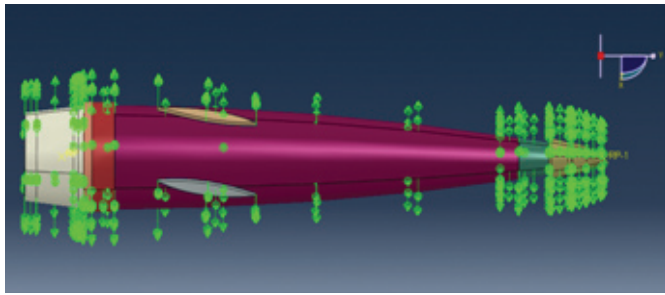


Figure 9. P-t curve acquired from the dynamic firing.

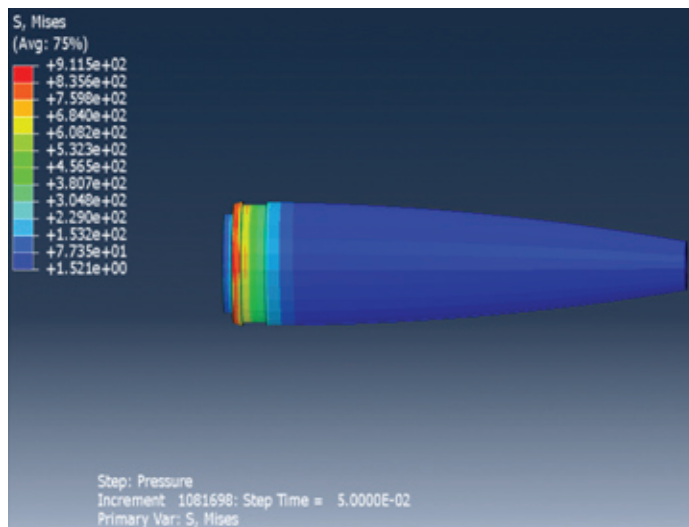


(a)

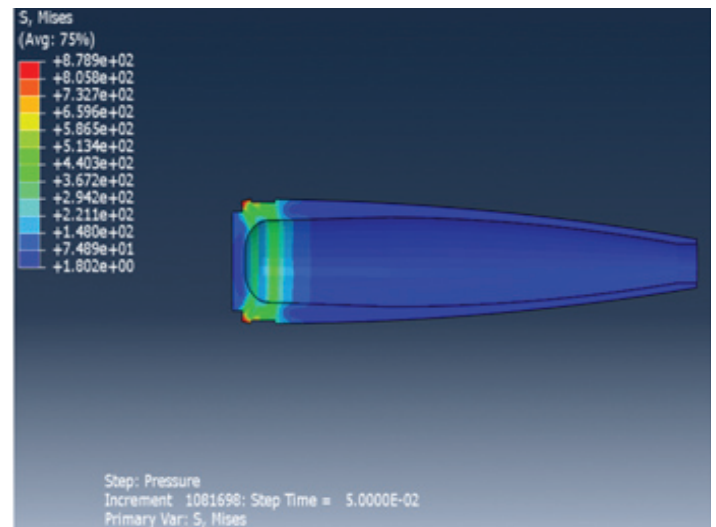


(b)

Figure 10. Loading on projectile 155mm ERFB BT: (a) Pressure, and (b) Spin.



(a)



(b)

Figure 11. von Mises stress plot:(a) Shell body, and (b) Cut section of shell body.

### 3. RESULTS

#### 3.1 von Mises Stress

Figures 11(a) and (b) show von Mises stress pattern of the shell body in which it is noticed that the most stressed region is located adjacent to the driving band near the projectile base. Stress concentration on the circumferential edge of the driving band seat is observed. The stress concentration is attributed to the change in the geometrical shape of the projectile body. The portion of the driving band seat has exhibited von Mises stress higher but below the yield strength of the shell body material. Figure 12(a) shows the stress concentration at the tommy holes and along the circumferential top edge of the boat tail. Figure 12(b) clearly displays high stressed driving band material.

#### 3.2 Plastic Strain

Figures 13(a) and (b) show the equivalent plastic strain (PEEQ) plot of the projectile. No plastic strain is observed in the shell body as well as in the boat tail. The driving band has exhibited plastic strain significantly, thus indicating plastic deformation.

The maximum values of von Mises stresses and equivalent plastic strains (PEEQ) observed in the projectile components are given in Table 2.

### 4. DISCUSSION

The von Mises stress pattern as shown in Figure 11 indicates the critical region of the projectile. The von Mises stress close to the driving band is observed more due to the geometrical discontinuity of the shell body. The contour plot of the PEEQ being the scalar measure has clearly shown the driving band as the most strained component of the shell assembly. This is attributed to the mechanical properties of the driving band material and the design stipulations based on the role of the driving band. The mounting of the driving band on the shell body is found intact which confirms the tightness of the driving band, which is in good agreement with the design stipulations.

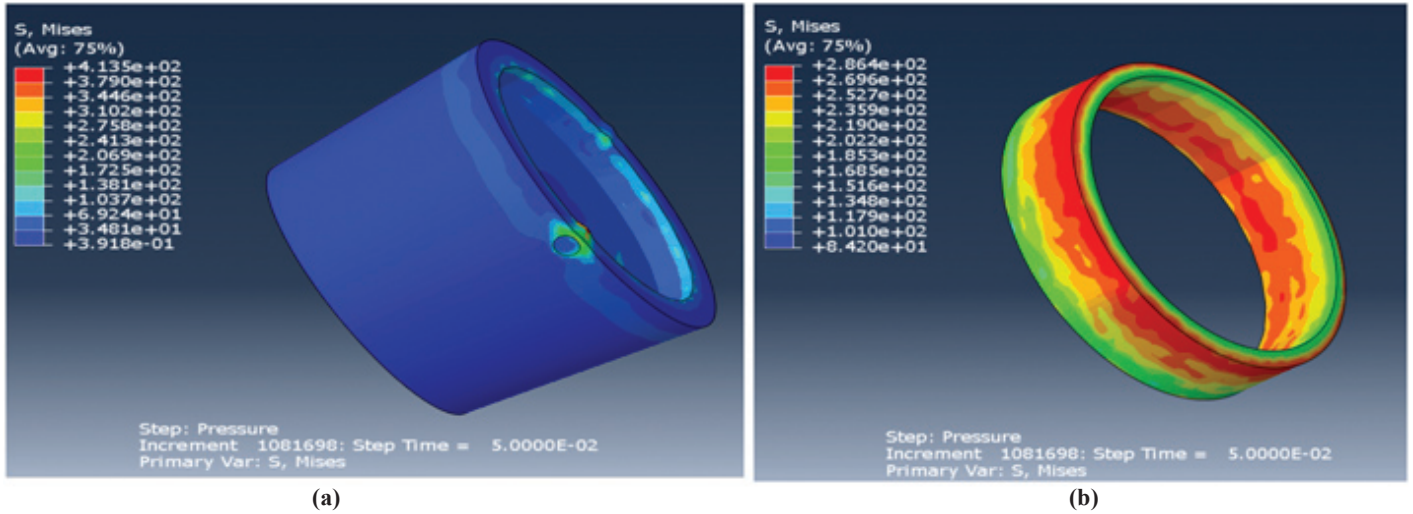


Figure 12. vonMises stress plots: (a) Boat tail, and (b) Driving band.

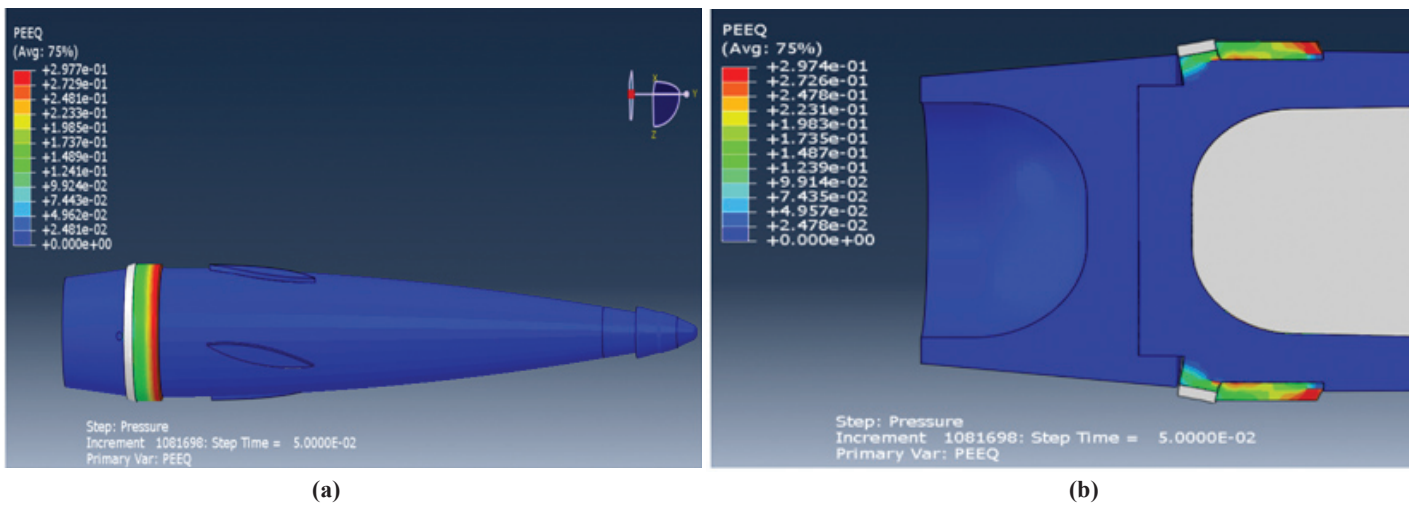


Figure 13. Equivalent Plastic Strain (PEEQ) plot: (a) Projectile 155 mm ERFB BT, and (b) Cut section of projectile 155 mm ERFB BT.

Table 2. Maximum values of von Mises stresses and PEEQ

Component	Maximum von Mises stress (MPa)	Maximum Equivalent Plastic Strain (PEEQ)
Shell Body	684.0	0.198
Boat Tail	413.5	0.099
Driving Band	286.4	0.298

5. CONCLUSIONS

A 3-D explicit dynamic analysis of shell 155 mm HE ERFB BT was carried out by finite element method using ABAQUS software. The structural integrity of projectile 155 mm high explosive ERFB boat tail subjected to complex gun-launch conditions was examined critically to check for any weakness in the design. The outcome of the analysis has proved to be useful in the investigation of the plastic deformation of the shell body, boat tail and affirmed that the projectile structure is capable of surviving gun launch at maximum propellant charge pressure. A 3-D explicit dynamic structural analysis has made it possible to look at the spectrum of loading conditions that the projectile is being exposed to. The following key conclusions have been drawn from the present investigational study.

- The geometric non-linearity of the shell body and the boat tail has been verified by knowing the deformation

of the shell assembly. The strain is observed only at the circumferential edge portion of the driving band seat and at the inner cavity portion of the boat tail. However, this strain does not contribute to any change in the diameter of the projectile.

- No stripping of the driving band has been observed. The PEEQ of the driving band material has been observed to be greater than zero, which establishes the yielding of the driving band material. The plastic deformation of the driving band material is desirable as per its functional role.
- The equivalent stress i.e. the von Mises stress at the bottom of the shell body is found comparatively more but within the yield limit. This is in good agreement with the design consideration that the maximum setback force of

the projectile is at the bottom of the shell body during gun launch.

- No plastic deformation of the shell body and boat tail has been noticed, thus affirming the structural integrity of the projectile inside the gun barrel.
- 3-D explicit dynamic analysis using von Mises plasticity model has revealed the plastic behavior of the projectile 155mm ERFB boat tail in a more comprehensive manner as compared to other methods.

## REFERENCES

1. AMC, Weapon systems and components. Elements of armament engineering, Part 3. USA, AMCP 706-108, 1963.
2. Wilkerson, Stephen; Hopkins, M.B. David & Gazonas, George. Developing a transient finite element model to simulate the launch environment of the 155-mm SADARM Projectile, Weapons and Materials Research Directorate, USA, Army Research Laboratory, Technical Report No. TR-ARL-2341, 2000.
3. Lindeman, R.A. Critical evaluation and stress analysis of the 5”/54 Hi-Frag projectile, U.S. Naval Weapons Laboratory, Technical Report No. TRW3164, 1974.
4. Drysdale, W.H. Design of kinetic energy projectiles for structural integrity, USA, Army Ballistic Research Laboratory, Aberdeen, MD, ARBRL Technical Report No. 02365, 1981.
5. Stephen, E.R.; Michael, J.N. & James, F. A. Study of projectile response to ballistics environment, USA, Army Research Laboratory, Technical Report No. TR-3672, 2005.
6. Swazek, S. Energetics and munitions suitability for gun launch. Insensitive munitions energetic material technology symposium, Spain. 2019.
7. Baker, E.L. & Michael, W.S. Gun launch and setback actuators. *In* Insensitive munitions energetic materials technology symposium, Portland OR, 2018.
8. Sadik, S. Final report on a study of premature explosions in artillery projectiles filled with composition-B, Lawrence Livermore Laboratory, University of California, Technical Report No. UCRL-53150, 1983.
9. Tien-Yu, T.; Chiesa, M. L. & Callabresei. Three dimensional stress analysis of an artillery projectile joint, Army Materials and Mechanics Research Center, Watertown MA, 1984.
10. Pflagl, G.A.; Underwood, J. H. & O’Hara, G.P. Structural analysis of a kinetic energy projectile during launch, USA, Army Armament Research and Development Command, Technical Report No. ARLCB-TR-81028, 1981.
11. Michael, S.L. Holis. Use of finite element stress analysis in the design of a tank cannon launched training projectile, USA, Army Research Laboratory, Technical Report No. TR-ARL-MR-149, 1994.
12. Pathak, K.K. & Jha, M. Structural analysis of a kinetic energy projectile for medium caliber gun. 19<sup>th</sup> International symposium of ballistics, Interlaken, Switzerland, 2001.
13. Balasubramanian, J.; Vasundhra, Ramesh, P.S. & Sivaramkrishnan, V. Finite element analysis of 125

mm tank gun smooth bore barrel behaviour during sand ingress, *Appl. Sci. Info. Sci. J.*, 2019, **13**(1), 81-86.

doi: 10.18576/amis/130111

14. Bender, J.M. & Reinhardt, L. E. A comparison of structural analysis techniques for the excalibur 155mm artillery shell’s canard actuation system, USA, Army Research Laboratory, Technical Report No. TR-3409, 2005.
15. Sorensen, B.R. Design and analysis of kinetic energy projectiles using finite element optimization, Aberdeen proving ground, MD, USA, Army Armament Research and Development Command, Ballistics Research Laboratory, Technical Report No. TR-3289, 1991.
16. ASTM E8/E8M-13a. Standard test methods for tension testing of metallic materials, ASTM International, 100 Barr Harbor Drive, P.O. Box C700, West Conshohocken, PA 19428-2959, USA, 2013.
17. Alan, F.L. Mechanics and mechanisms of fracture: An introduction, ASM International, Ohio, 2005. 15p.
18. Carlucci, D.E. & Jacobson, S. S. Ballistics: theory and design of guns and ammunition, CRC Press, Boca Raton, USA, 2018.
19. Ruth, C.R. & Evans, J.W. A short-barrelled 105mm howitzer for interior ballistic studies, USA, Army Armament Research and Development Command, Ballistic Research Laboratory, Memorandum Report No. ARBRL-MR-03238, 1983.

## ACKNOWLEDGMENT

Authors are thankful to the Vice Chancellor, DIAT, Deemed University, Pune for allowing this research study at DIAT (DU), Pune. Authors would like to thank Mr Tekram Parshuramkar for providing the help in conducting the experiments for this research work. Authors also wish to express their gratitude for CAE support provided by Mr Narendra Palande.

## CONTRIBUTORS

**Mr Rajesh B. Ohol** is Master of Technology in Armament and Combat Vehicles from Defence Institute of Advanced Technology (Deemed University), Pune. He has been working as Assistant Engineer (Quality Assurance) in Directorate General of Quality Assurance, Ministry of Defence, Government of India. Currently, he is pursuing PhD in Failure analysis of artillery ammunition from Defence Institute of Advanced Technology. His area of research includes armament engineering and defect investigation of ammunitions.

In this paper, he did the literature survey, performed the experiments, numerical analysis and interpretation of results and prepared the manuscript.

**Dr B.A. Parate**, Scientist ‘F’, is working at ARDE. He obtained PhD in Mechanical Engg from DIAT, Pune in the year 2020. His doctoral research is based on ‘Experimental and Analytical Analysis of Water-Jet Disruptor’. Till date he has published 56 papers. He has guided many students of BE and ME for completion of various projects. In this paper, he guided the author and reviewed the manuscript.

**Dr Dineshsingh G. Thakur** obtained Master of Technology in Mechanical Engineering and PhD from Indian Institute of Technology, Madras. His research domains are CAD/CAM/Robotics, Manufacturing Consideration in Design, High-Speed Machining/Green Machining of Aerospace Materials, Precision Robotic Welding of Aerospace Materials, Micro-manufacturing/Micromachining of ‘difficult to cut

materials’. Presently, he is the Head of the Department of Mechanical Engineering in Defence Institute of Advanced Technology (Deemed University), Pune (India). He has published a good number of research papers in the International Journals. In the present work, he guided the author, reviewed and formatted the manuscript.